

## APPLICATION OF CALCINED LAYERED DOUBLE HYDROXIDES AS CATALYSTS FOR ABATEMENT OF N<sub>2</sub>O EMISSIONS

Lucie OBALOVÁ<sup>a1,\*</sup>, František KOVANDA<sup>b</sup>, Květuše JIRÁTOVÁ<sup>c</sup>,  
Kateřina PACULTOVÁ<sup>a</sup> and Zdenek LACNÝ<sup>a</sup>

<sup>a</sup> Technical University of Ostrava, 17. listopadu 15, 708 33 Ostrava, Czech Republic;  
e-mail: <sup>1</sup> lucie.obalova@vsb.cz

<sup>b</sup> Department of Solid State Chemistry, Institute of Chemical Technology, Prague,  
Technická 5, 166 28 Prague 6, Czech Republic; e-mail: frantisek.kovanda@vscht.cz

<sup>c</sup> Institute of Chemical Process Fundamentals, Academy of Sciences of the Czech Republic, v.v.i.,  
Rozvojová 135, 165 02 Prague 6, Czech Republic; e-mail: jiratova@icpf.cas.cz

Received April 30, 2008

Accepted August 1, 2008

Published online October 3, 2008

The results of catalytic decomposition of N<sub>2</sub>O over mixed oxide catalysts obtained by calcination of layered double hydroxides (LDHs) are summarized. Mixed oxides were prepared by thermal treatment (500 °C) of coprecipitated LDH precursors with general chemical composition of M<sup>II</sup><sub>1-x</sub>M<sup>III</sup><sub>x</sub>(OH)<sub>2</sub>(CO<sub>3</sub>)<sub>x/2</sub>·yH<sub>2</sub>O, where M<sup>II</sup> was Ni, Co, Cu and/or Mg, M<sup>III</sup> was Mn, Fe and/or Al, and the M<sup>II</sup>/M<sup>III</sup> molar ratio was adjusted to 2. The influence of chemical composition of the M<sup>II</sup>-M<sup>III</sup> mixed oxide catalysts on their activity and stability in N<sub>2</sub>O decomposition was examined. The highest N<sub>2</sub>O conversion was reached over Ni-Al (4:2) and Co-Mn-Al (4:1:1) catalysts. Their suitability for practical application was proved in simulated process stream in the presence of O<sub>2</sub>, NO, NO<sub>2</sub> and H<sub>2</sub>O. It was found that N<sub>2</sub>O conversion decreased with increasing amount of oxygen in the feed. The presence of NO in the feed caused a slight decrease in N<sub>2</sub>O conversion. A strong decrease in the reaction rate was observed over the Ni-Al catalyst in the presence of NO<sub>2</sub> while no N<sub>2</sub>O conversion decrease was observed over the Co-Mn-Al catalyst. Water vapor inhibited the N<sub>2</sub>O decomposition over all tested catalysts. The obtained kinetic data for N<sub>2</sub>O decomposition in a simulated process stream over the Co-Mn-Al catalyst were used for a preliminary reactor design. The packed bed volume necessary for N<sub>2</sub>O emission abatement in a HNO<sub>3</sub> production plant was calculated as 35 m<sup>3</sup> for waste gas flow rate of 30 000 m<sup>3</sup> h<sup>-1</sup>.

**Keywords:** Nitrous oxide; Catalytic decomposition; Mixed oxides; Layered double hydroxides; Inhibition.

Nitrous oxide (N<sub>2</sub>O) belongs to a group of compounds depleting stratospheric ozone layer and also strongly contributes to the greenhouse effect. Nitric acid plants are indicated as the biggest industrial source of anthropogenic N<sub>2</sub>O emissions (worldwide 400 kt N<sub>2</sub>O per year)<sup>1</sup>. Nitrous oxide to-

gether with nitrogen arises from non-selective oxidation of ammonia during high-temperature  $\text{NH}_3$  oxidation over Pt-Rh sieves, possibly by consecutive reactions of NO and nonreacted ammonia<sup>1-3</sup>.

One of the possible methods for  $\text{N}_2\text{O}$  emission lowering is direct  $\text{N}_2\text{O}$  decomposition according to Eq. (1).



Reaction (1) represents a spin-forbidden reaction with high activation energy (250–270  $\text{kJ mol}^{-1}$ ); a measurable  $\text{N}_2\text{O}$  conversion could be obtained only above 620 °C. On the other hand, 100%  $\text{N}_2\text{O}$  conversion could be obtained already at 320 °C in the presence of a suitable catalyst, depending on the composition of inlet gas. It is known that water vapour, oxygen and possibly other components characteristic of off-gases containing  $\text{N}_2\text{O}$  have inhibition effect over some of the catalysts<sup>4-7</sup>.

The reaction rate of  $\text{N}_2\text{O}$  decomposition according to Eq. (1) could be further increased in the presence of a reducing agent (such as hydrocarbons, ammonia or carbon monoxide)<sup>8-22</sup>. A reducing agent added into the inlet gas decreases the temperature necessary for full  $\text{N}_2\text{O}$  conversion; however, it increases operating costs of the process and undesirable reaction products can be formed. Therefore, the catalysts should exhibit also a satisfactory selectivity.

A sufficiently active and stable catalyst is still the object of the research despite the fact that many catalysts have been tested for  $\text{N}_2\text{O}$  decomposition or reduction<sup>4,23</sup>. The present work deals with the  $\text{N}_2\text{O}$  catalytic decomposition over mixed oxides prepared by thermal decomposition of layered double hydroxides.

Layered double hydroxides (LDHs), known also as hydrotalcite-like compounds or anionic clays, are layered materials consisting of positively charged hydroxide layers separated by interlayers composed of anions and water molecules. The chemical composition of LDHs can be represented by the general formula  $[\text{M}^{\text{II}}_{1-x}\text{M}^{\text{III}}_x(\text{OH})_2]^{x+}[\text{A}^{n-}_{x/n}\text{yH}_2\text{O}]^{x-}$  where  $\text{M}^{\text{II}}$  and  $\text{M}^{\text{III}}$  are divalent and trivalent metal cations,  $\text{A}^{n-}$  is an  $n$ -valent anion, and  $x$  has usually values between 0.20 and 0.33. A wide variety of LDHs can be prepared modifying both the composition of hydroxide layers and interlayer species. After heating at moderate temperatures, LDHs give finely dispersed mixed oxides of  $\text{M}^{\text{II}}$  and  $\text{M}^{\text{III}}$  metals with a large surface area and good thermal stability<sup>24-29</sup>. Therefore, the LDHs are often used as precursors for preparation of mixed oxide catalysts. Some of them were also tested in the catalytic decomposition of nitrous oxide<sup>30-41</sup>.

The effect of chemical composition of mixed-oxide catalysts on their catalytic activity for  $N_2O$  decomposition was studied in the present work. The catalyst testing in inert gas was carried out in order to compare the activity of catalysts containing various  $M^{II}$  and  $M^{III}$  metals. The tests in a simulated process stream (in the presence of  $O_2$ ,  $NO$ ,  $NO_2$  and  $H_2O$ ) were performed in order to elucidate a practical application of selected catalysts, over which a high  $N_2O$  conversion was obtained. Based on the results, some parameters of a catalytic reactor for  $N_2O$  emission abatement from nitric acid production plant were estimated.

## EXPERIMENTAL

The LDH precursors with chemical composition represented by general formula  $[M^{II}_{1-x}M^{III}_x(OH)_2(CO_3)_{x/2} \cdot yH_2O]$ , where  $M^{II} = Ni, Co, Cu$  and/or  $Mg$ , and  $M^{III} = Mn, Fe$  and/or  $Al$  were prepared by coprecipitation. An aqueous solution (450 ml) of appropriate nitrates, i.e.,  $Ni(NO_3)_2 \cdot 6H_2O$ ,  $Co(NO_3)_2 \cdot 6H_2O$ ,  $Cu(NO_3)_2 \cdot 3H_2O$ ,  $Mg(NO_3)_2 \cdot 6H_2O$ ,  $Mn(NO_3)_2 \cdot 4H_2O$ ,  $Fe(NO_3)_3 \cdot 9H_2O$  and  $Al(NO_3)_3 \cdot 9H_2O$ , with a  $M^{II}/M^{III}$  molar ratio of 2 and total metal ion concentration  $1.0 \text{ mol l}^{-1}$  was added with flow rate of  $7.5 \text{ ml min}^{-1}$  into 1000 ml reactor containing 200 ml of distilled water. The flow rate of simultaneously added alkaline solution of  $0.5 \text{ M Na}_2CO_3$  and  $3 \text{ M NaOH}$  was controlled to maintain reaction pH at  $10.0 \pm 0.1$ . The coprecipitation was carried out under vigorous stirring at  $30 \text{ }^\circ\text{C}$ . The resulting suspension was stirred at  $30 \text{ }^\circ\text{C}$  for 1 h, the obtained product was then filtered off, washed thoroughly with distilled water, and dried overnight at  $60 \text{ }^\circ\text{C}$  in air. The dried precursors were formed into extrudates and calcined in air at  $500 \text{ }^\circ\text{C}$  for 4 h. The calcined extrudates were crushed and sieved to obtain the fraction with particle size  $0.160\text{--}0.315 \text{ mm}$ . The prepared catalysts were denoted by acronyms with elemental composition and the molar ratios of the constituents. For example,  $Co_4MnAl$  sample contained  $Co, Mn$  and  $Al$  in molar ratio of 4:1:1.

The prepared precursors and mixed oxide catalysts were characterized by chemical analysis, powder X-ray diffraction (XRD), infrared (IR), photoelectron (XPS) and Raman spectroscopy and by surface area measurements. Details of the used methods are described in our previous reports<sup>42–44</sup>.

The  $N_2O$  catalytic reaction was performed in a fixed-bed reactor (i.d. 5 mm) in the temperature range  $300\text{--}450 \text{ }^\circ\text{C}$  with the total flow rate  $50\text{--}330 \text{ ml min}^{-1}$  NTP (273 K, 101.325 kPa),  $0.1\text{--}0.33 \text{ g}$  of catalyst and a space velocity of  $30\text{--}60 \text{ l h}^{-1}\text{g}^{-1}$ . Inlet concentration was varied according to the type of experiment in the following range:  $0\text{--}0.1 \text{ mole } \%$   $N_2O$ ,  $0\text{--}20 \text{ mole } \%$   $O_2$ ,  $0\text{--}0.17 \text{ mole } \%$   $NO_2$ ,  $0\text{--}0.17 \text{ mole } \%$   $NO$  and  $0\text{--}3 \text{ mole } \%$   $H_2O$  balanced by helium. All the measurements were carried out at a steady state.

A gas chromatograph Agilent Technologies 6890 N with TCD detector was used to measure  $N_2O$ ,  $O_2$  and  $N_2$  concentrations. The valve system made it possible to switch the columns Poraplot Q  $30 \text{ m} \times 0.53 \text{ mm} \times 40 \text{ } \mu\text{m}$  for separation of  $N_2O$  and Molsieve 5A  $30 \text{ m} \times 0.53 \text{ mm} \times 25 \text{ } \mu\text{m}$  for separation of  $N_2$  and  $O_2$ .  $NO$  and  $NO_2$  were determined by an IR analyzer Ultramat 6 (Siemens) supplemented by a catalytic  $NO_2/NO$  converter (TESO). Water vapor was added via a saturator with a Nafion® (Perma Pure Inc.) membrane. The moisture content was controlled by measuring relative humidity and temperature (Thermo).

## RESULTS AND DISCUSSION

*Catalyst Characterization*

Physico-chemical properties of the selected catalysts are summarized in Table I. In all cases, the LDH precursors were transformed into mixed oxides by calcination at 500 °C. Release of interlayer water, dehydroxylation of hydroxide layers and decomposition of interlayer carbonate resulted in evolution of a large amount of volatile components (H<sub>2</sub>O and CO<sub>2</sub>) and destruction of the layered LDH structure. The formation of oxide phases was confirmed by XRD and Raman spectroscopy. The FTIR spectroscopy revealed a slight amount of residual carbonate in some calcined samples.

Simple M<sup>II</sup>O oxides were found by XRD in the calcined M<sup>II</sup>-Al samples (Ni<sub>4</sub>Al<sub>2</sub> and Cu<sub>4</sub>Al<sub>2</sub>); no individual Al-containing crystalline phase was detected in these catalysts. A mixed oxide with spinel structure, which could be considered as a solid solution of Co<sub>3</sub>O<sub>4</sub> and CoAl<sub>2</sub>O<sub>4</sub> spinels, was identified in the powder XRD pattern of the Co<sub>4</sub>Al<sub>2</sub> sample. Non-stoichiometric

TABLE I  
Catalyst characterization

Catalyst	Crystalline phase (XRD)	$S_{\text{BET}}/\text{m}^2\text{g}^{-1}$	M <sup>II</sup> /M <sup>III</sup> molar ratio <sup>a</sup>	
			Bulk (AAS)	Surface (XPS)
Mg <sub>4</sub> Mn <sub>2</sub>	Mg <sub>6</sub> MnO <sub>8</sub>	52	2.00	2.20
Mg <sub>4</sub> Fe <sub>2</sub>	MgO, Fe <sub>3</sub> O <sub>4</sub> /Fe <sub>2</sub> O <sub>3</sub>	98	2.00	n.d. <sup>b</sup>
Co <sub>4</sub> Al <sub>2</sub>	Co <sub>3</sub> O <sub>4</sub> , CoAl <sub>2</sub> O <sub>4</sub>	86	1.92	0.64
Co <sub>4</sub> MnAl	Co <sub>3</sub> O <sub>4</sub> , Co-Al-Mn spinel	93	Co/Mn 4.12 Co/Al 3.85	Co/Mn 2.38 Co/Al 1.97
Co <sub>4</sub> Mn <sub>2</sub>	Co <sub>3</sub> O <sub>4</sub> , Co-Mn spinel	76	2.00	0.9–1.2
Co <sub>4</sub> Fe <sub>2</sub>	Co-Fe spinel	44	2.00	n.d.
Ni <sub>4</sub> Al <sub>2</sub>	NiO	188	1.96	2.06
Ni <sub>4</sub> Mn <sub>2</sub>	Ni <sub>6</sub> MnO <sub>8</sub> , NiMnO <sub>3</sub>	72	1.92	n.d.
Ni <sub>4</sub> Fe <sub>2</sub>	Ni-Fe spinel	69	2.00	n.d.
Cu <sub>4</sub> Al <sub>2</sub>	CuO	47	2.08	0.70
Cu <sub>4</sub> Mn <sub>2</sub>	CuO, Cu-Mn spinel	48	2.02	n.d.

<sup>a</sup> M<sup>II</sup> = Co, Ni, Cu, Mg; M<sup>III</sup> = Al, Mn, Fe. <sup>b</sup> n.d., not determined.

oxides with spinel structure were found also in other samples containing cobalt<sup>45</sup>. Only spinel-type mixed oxides were found also in the Fe-containing samples ( $\text{Ni}_4\text{Fe}_2$  and  $\text{Co}_4\text{Fe}_2$ ); iron oxides  $\text{Fe}_3\text{O}_4$  and/or  $\text{Fe}_2\text{O}_3$  together with MgO were detected in the  $\text{Mg}_4\text{Fe}_2$  sample. The Mn-containing catalysts exhibited very different phase compositions. As it was mentioned above, in the Co-containing samples ( $\text{Co}_4\text{Mn}_2$  and  $\text{Co}_4\text{MnAl}$ ) only spinel-type oxides were found. In the  $\text{Cu}_4\text{Mn}_2$  sample, Cu-Mn spinel together with CuO was detected. Murdochite-like mixed oxides containing  $\text{Mn}^{\text{IV}}$ ,  $\text{Mg}_6\text{MnO}_8$  and  $\text{Ni}_6\text{MnO}_8$  were identified in the  $\text{Mg}_4\text{Mn}_2$  and  $\text{Ni}_4\text{Mn}_2$  samples, respectively. In the  $\text{Ni}_4\text{Mn}_2$  catalyst, the  $\text{NiMnO}_3$  oxide with ilmenite structure was detected together with  $\text{Ni}_6\text{MnO}_8$ <sup>46</sup>. A certain content of amorphous part was found together with crystalline phases in all examined catalysts.

A surface area ranging from 44 to 188  $\text{m}^2 \text{g}^{-1}$  was measured with the examined catalysts, which can be explained by evolution of volatile components and formation of porous structure during calcination of LDH precursors. Surface composition of some catalysts determined by photoelectron spectroscopy was different from the bulk one. An enrichment of the catalyst surface in Al and/or Mn was observed. An exception to this trend was observed with  $\text{Ni}_4\text{Al}_2$  sample, in which no difference between the surface and bulk composition was found.

### *Catalytic Decomposition of $\text{N}_2\text{O}$ in Inert Gas*

The temperature dependence of  $\text{N}_2\text{O}$  conversion in an inert gas was used in order to compare the catalytic activity of catalysts with different chemical composition (Fig. 1). Nitrous oxide decomposition over some catalysts ( $\text{Ni}_4\text{Al}_2$ ,  $\text{Co}_4\text{Al}_2$ ,  $\text{Cu}_4\text{Al}_2$ ) has been already reported by other authors<sup>47,48</sup> and the obtained results were comparable with the published data. The other examined catalysts contained two transition metal cations or transition metal cations in combination with  $\text{Mg}^{2+}$ . These mixed oxides have not been tested in  $\text{N}_2\text{O}$  decomposition so far. A combination of two transition metals in  $\text{Co}_4\text{Mn}_2$ ,  $\text{Cu}_4\text{Mn}_2$  and  $\text{Co}_4\text{Fe}_2$  catalysts enhanced the  $\text{N}_2\text{O}$  decomposition in comparison with analogous  $\text{M}^{\text{II}}\text{-Al}$  catalysts. On the other hand, a decrease in catalytic activity was observed with  $\text{Ni}_4\text{Mn}_2$  and  $\text{Ni}_4\text{Fe}_2$  samples. Out of the group of mixed oxide catalysts containing three-cation components<sup>42-44</sup>, only the most active  $\text{Co}_4\text{MnAl}$  sample is mentioned in this study.

The XPS and TPR results published recently<sup>44-46</sup> indicate that optimization of physico-chemical properties of the mixed oxides can give catalysts

active in  $N_2O$  decomposition. As it implies from published mechanisms of  $N_2O$  decomposition, an optimum oxygen bond strength is supposedly a prerequisite for a very active  $N_2O$  decomposition catalyst<sup>4</sup>. The oxygen bond strength can be determined from TPR experiment as a shift of reduction peak maximum to lower temperatures. The  $H_2$  consumption in the temperature range from 350 to 450 °C was chosen as the parameter of oxygen bond strength on the catalyst surface. The optimal value of  $H_2$  consumption in the selected interval corresponding to the highest catalytic activity was found. It was also found that such catalysts contain an optimum amount of metal components in suitable oxidation state<sup>44</sup>.

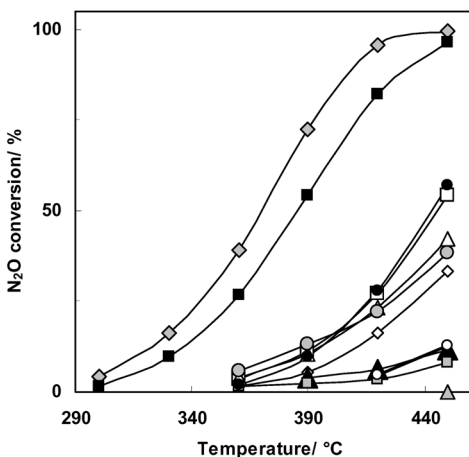


FIG. 1

Temperature dependence of  $N_2O$  conversion over  $Ni_4Al_2$  ( $\blacklozenge$ ),  $Cu_4Al_2$  ( $\diamond$ ),  $Co_4MnAl$  ( $\blacksquare$ ),  $Co_4Mn_2$  ( $\square$ ),  $Ni_4Mn_2$  ( $\blacksquare$ ),  $Cu_4Mn_2$  ( $\blacktriangle$ ),  $Co_4Al_2$  ( $\triangle$ ),  $Mg_4Fe_2$  ( $\blacktriangle$ ),  $Co_4Fe_2$  ( $\bullet$ ),  $Ni_4Fe_2$  ( $\circ$ ) and  $Mg_4Mn_2$  ( $\bullet$ ) catalysts. Conditions: 0.1 mole %  $N_2O$ , 0.1 g,  $100\text{ ml min}^{-1}$

### *Catalytic Decomposition of $N_2O$ in Simulated Process Stream*

The  $Ni_4Al_2$  and  $Co_4MnAl$  catalysts, exhibiting the highest activity in the preliminary tests performed in an inert gas, were chosen for testing  $N_2O$  decomposition in the presence of other gaseous components, which could simulate a real off-gas in industrial plants. A mixture containing oxygen, water vapor, NO and  $NO_2$  together with  $N_2O$  (~1000 ppm) was used as a model gas for catalyst testing; the chosen composition corresponded to the waste gas from nitric acid production plant.

The effect of  $O_2$  and  $NO_2$  addition on the  $N_2O$  conversion obtained over the  $Ni_4Al_2$  and  $Co_4MnAl$  catalysts is shown in Figs 2 and 3. The  $N_2O$  conversion decreased with increasing amount of oxygen in the inlet: a sharp

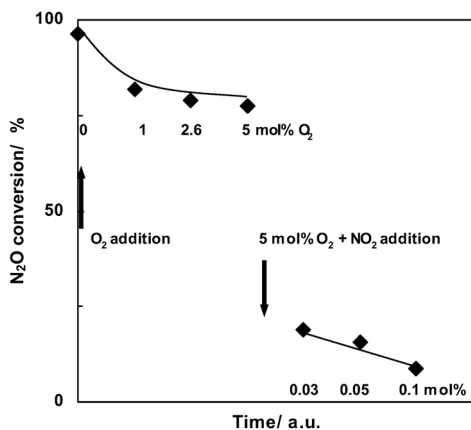


FIG. 2

Effect of  $O_2$  and  $NO_2$  addition on the  $N_2O$  conversion over  $Ni_4Al_2$  at 450 °C. Conditions: 0.1 mole %  $N_2O$ , 0.2 g, 50 ml  $min^{-1}$ , 450 °C

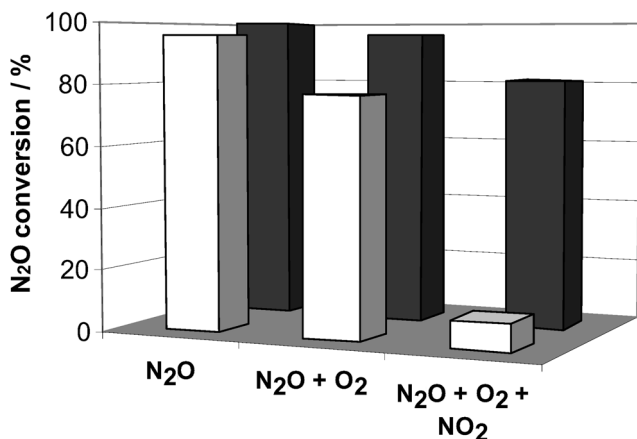


FIG. 3

Effect of  $O_2$  and  $NO_2$  addition on  $N_2O$  conversion at 450 °C over  $Co_4MnAl$  (■) and  $Ni_4Al_2$  (□) catalysts. Conditions: 0.1 mole %  $N_2O$ , 5 mole %  $O_2$ , 0.1 mole %  $NO_2$ .  $Ni_4Al_2$ : 0.2 g, 50 ml  $min^{-1}$ ;  $Co_4MnAl$ : 0.3 g, 100 ml  $min^{-1}$

decrease was observed up to 2 mole % O<sub>2</sub> over the Ni<sub>4</sub>Al<sub>2</sub> catalyst, while further addition of oxygen did not cause any other conversion decrease – the conversion remained nearly constant (Fig. 2). Comparison of N<sub>2</sub>O conversion over the examined catalysts measured in the presence of 5 mole % O<sub>2</sub> is shown in Fig. 3. In spite of the different space velocity applied, it is evident that the Co<sub>4</sub>MnAl catalysts exhibited a lower decrease in N<sub>2</sub>O conversion in comparison with Ni<sub>4</sub>Al<sub>2</sub>.

The examined catalysts exhibited a different change in N<sub>2</sub>O conversion after NO<sub>2</sub> addition. A considerable decrease in N<sub>2</sub>O conversion was observed over the Ni<sub>4</sub>Al<sub>2</sub> catalyst (see Fig. 2), the N<sub>2</sub>O conversion being further decreased with increasing NO<sub>2</sub> concentration. The decrease in N<sub>2</sub>O conversion can be likely caused by NO<sub>2</sub> competitive adsorption on the active sites. Over the Co<sub>4</sub>MnAl catalyst, a much lower inhibition effect of NO<sub>2</sub> addition was found (see Fig. 3).

The effect of water vapor addition on the N<sub>2</sub>O conversion was tested over the Ni<sub>4</sub>Al<sub>2</sub>, Co<sub>4</sub>Al<sub>2</sub>, Co<sub>4</sub>MnAl and Co<sub>4</sub>Mn<sub>2</sub> catalysts with the aim to elucidate the reversibility of the water vapor inhibition effect (Figs 4 and 5).

As the N<sub>2</sub>O conversion was irreversibly decreased in the presence of water vapor over the Ni<sub>4</sub>Al<sub>2</sub> catalyst, the attention was focused on the catalysts containing Co, Mn and Al<sup>43,44</sup>. Over all examined catalysts water vapor in

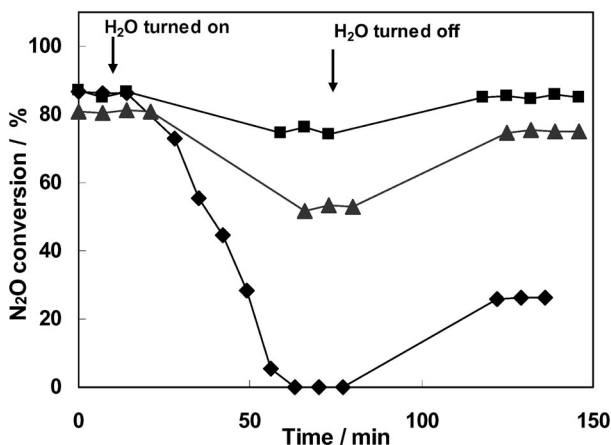


FIG. 4

Effect of water vapor addition on the N<sub>2</sub>O conversion over Ni<sub>4</sub>Al<sub>2</sub> (◆), Co<sub>4</sub>Mn<sub>2</sub> (■) and Co<sub>4</sub>Al<sub>2</sub> (▲) catalyst. Conditions: 0.1 mole % N<sub>2</sub>O + 0.5 mole % H<sub>2</sub>O, 0.3 g, 100 ml min<sup>-1</sup>, 450 °C



the feed gas decreased the  $\text{N}_2\text{O}$  conversion (see Fig. 5), which further decreased with increasing concentration of water vapor (not shown here). However, a different drop in  $\text{N}_2\text{O}$  conversion was observed for individual catalysts. The highest  $\text{N}_2\text{O}$  conversion in the presence of water vapor was measured with the  $\text{Co}_4\text{MnAl}$  catalyst.

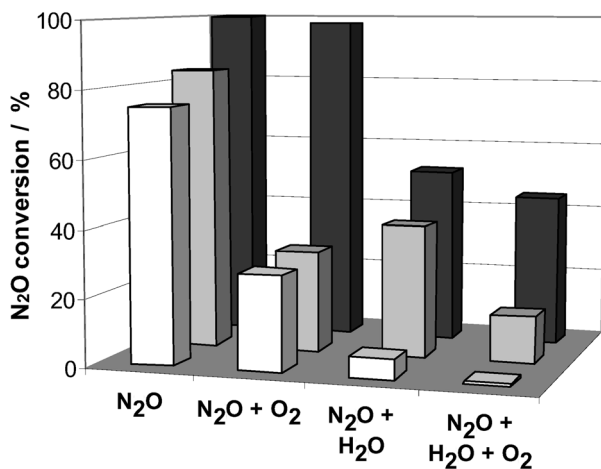


FIG. 5

Effect of water vapor and  $\text{O}_2$  addition on the  $\text{N}_2\text{O}$  conversion over  $\text{Co}_4\text{MnAl}$  (■),  $\text{Co}_4\text{Mn}_2$  (▒) and  $\text{Co}_4\text{Al}_2$  (□) catalysts. Conditions: 0.1 mole %  $\text{N}_2\text{O}$  + 0.5 mole %  $\text{H}_2\text{O}$ , 0.3 g, 100 ml  $\text{min}^{-1}$ , 450 °C

The effect of  $\text{NO}$  addition on the  $\text{N}_2\text{O}$  catalytic decomposition over the  $\text{Co}_4\text{MnAl}$  catalyst is shown in Fig. 6. The presence of  $\text{NO}$  in the feed caused a slight decrease in  $\text{N}_2\text{O}$  conversion and the conversion drop increased with increasing amount of  $\text{NO}$  in the gas inlet. The simultaneous presence of  $\text{NO}$  and  $\text{O}_2$  in the gas inlet resulted in a further very slight decrease in  $\text{N}_2\text{O}$  conversion, probably caused by formation of surface nitrates and nitrites and/or by consecutive reactions.

### Stability of the Catalysts

Gradual deactivation of the  $\text{Ni}_4\text{Al}_2$ ,  $\text{Co}_4\text{Al}_2$ ,  $\text{Ni}_2\text{Mg}_2\text{Al}_2$ ,  $\text{Co}_4\text{Mn}_2$  and  $\text{Co}_4\text{MnAl}$  catalysts was observed during long-term stability tests (Figs 7 and 8), while a slight gradual increase in  $\text{N}_2\text{O}$  conversion was observed over the  $\text{Mg}_4\text{Mn}_2$  catalyst during the testing period (see Fig. 7).

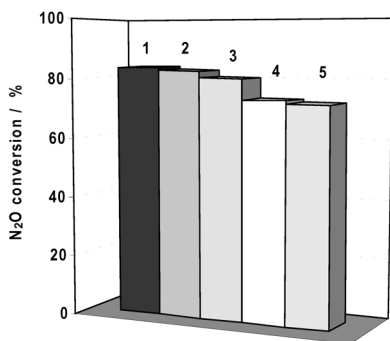


FIG. 6

Effect of NO and O<sub>2</sub> addition on the N<sub>2</sub>O catalytic decomposition over the Co<sub>4</sub>MnAl catalyst. Conditions: 1000 ppm N<sub>2</sub>O, 0.33 g, 330 ml min<sup>-1</sup>, 450 °C. Inlet mixture: N<sub>2</sub>O (1), N<sub>2</sub>O + 0.02 mole % NO (2), N<sub>2</sub>O + 0.06 mole % NO (3), N<sub>2</sub>O + 0.02 mole % NO + 4 mole % O<sub>2</sub> (4), N<sub>2</sub>O + 0.06 mole % NO + 4 mole % O<sub>2</sub> (5)

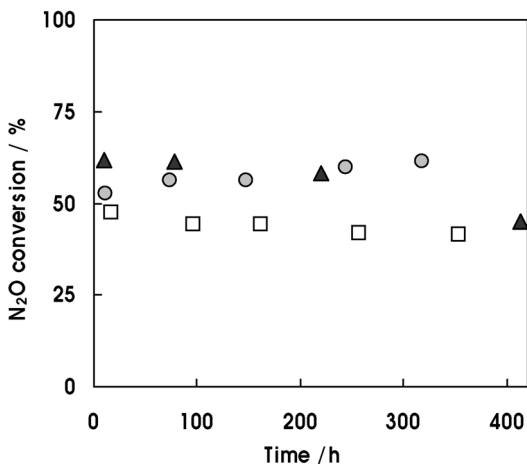


FIG. 7

Time dependence of N<sub>2</sub>O conversion over Co<sub>4</sub>Al<sub>2</sub> (□), Co<sub>4</sub>Fe<sub>2</sub> (▲) and Mg<sub>4</sub>Mn<sub>2</sub> (●) catalysts. Conditions: 0.1 mole % N<sub>2</sub>O, 450 °C. Co<sub>4</sub>Al<sub>2</sub>: 0.1 g, 100 ml min<sup>-1</sup>; Mg<sub>4</sub>Mn<sub>2</sub>: 0.2 g, 100 ml min<sup>-1</sup>; Co<sub>4</sub>Fe<sub>2</sub>: 0.33 g, 330 ml min<sup>-1</sup>

The most noticeable decrease in  $N_2O$  conversion was observed over the  $Co_4MnAl$  catalyst (see Fig. 8). The  $N_2O$  conversion decreased by 30 % during the first 300 h, but remained relatively constant in the course of the next 1200 h. The initial decrease in  $N_2O$  conversion can be likely caused by testing the catalyst under “the most aggressive” conditions – the sample was frequently cooled and heated and also exposed to various combinations of compounds such as  $O_2$ ,  $CO$ ,  $NO$ ,  $CO_2$  and  $NH_3$ .

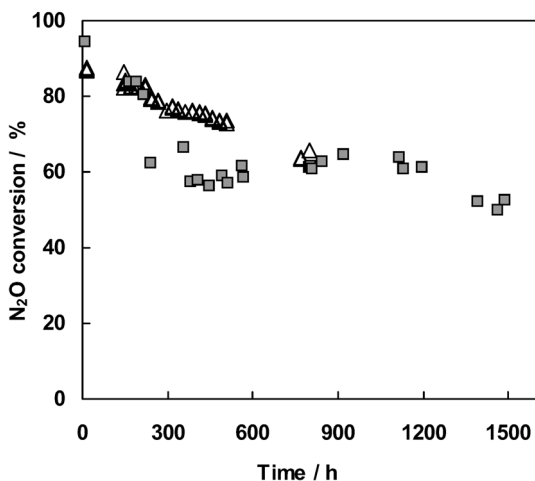


FIG. 8

Time dependence of  $N_2O$  conversion over  $Co_4Mn_2$  ( $\Delta$ ) and  $Co_4MnAl$  ( $\blacksquare$ ) catalysts. Conditions: 0.1 mole %  $N_2O$ , 450 °C.  $Co_4MnAl$ : 0.33 g, 330 ml  $min^{-1}$ ;  $Co_4Mn_2$ : 0.1 g, 100 ml  $min^{-1}$

The changes in catalyst activity reflect changes in both porous structure and surface concentration of active species (Table II). The lower thermal stability could be explained also by only a slight difference between the temperature, at which long-term catalytic measurements were performed (450 °C), and the temperature used for preparation of catalysts (the LDH precursors were calcined at 500 °C).

#### *Estimation of Parameters of Industrial Catalytic Unit for $N_2O$ Emission Abatement*

Based on the laboratory results obtained with the  $Co_4MnAl$  catalyst in simulated process stream conditions, dimensions of a catalytic unit for abate-

ment of N<sub>2</sub>O emissions from the nitric acid plant were calculated. Suitable position for the catalytic unit is at such a place<sup>49</sup> where NH<sub>3</sub> is not present in the gas stream in order to exclude a non-selective oxidation of ammonia to N<sub>2</sub>O, NO and NO<sub>2</sub>.

TABLE II  
Catalyst characterization of fresh catalysts and catalysts used in N<sub>2</sub>O decomposition

Catalyst	S <sub>BET</sub> , m <sup>2</sup> g <sup>-1</sup>		Surface composition, XPS	
	fresh	used	fresh	used
Mg <sub>4</sub> Mn <sub>2</sub>	52	36	Mn <sub>1</sub> Mg <sub>2.00</sub> Na <sub>0.35</sub> O <sub>5.06</sub>	Mn <sub>1</sub> Mg <sub>2.40</sub> Na <sub>0.52</sub> O <sub>4.47</sub>
Co <sub>4</sub> Mn <sub>2</sub>	76	62	Mn <sub>1</sub> Co <sub>0.9-1.2</sub> O <sub>4.80</sub>	Mn <sub>1</sub> Co <sub>0.9-1.2</sub> O <sub>4.90</sub>
Co <sub>4</sub> MnAl	93	n.d.	Mn <sub>1</sub> Co <sub>2.57</sub> Al <sub>1.35</sub> O <sub>9.59</sub>	Mn <sub>1</sub> Co <sub>1.89</sub> Al <sub>1.32</sub> O <sub>7.93</sub>

The reactor is proposed as a fixed-bed reactor with an ideal plug flow. The influence of internal and external diffusion was described by the overall effectiveness factor. The influence of external heat transfer on the reaction rate was neglected; under the given conditions, the catalyst particle is assumed as isothermal. The isothermal regime of the reactor was considered because of a low N<sub>2</sub>O concentration and consequently, a low amount of released heat.

Only a slight decrease of N<sub>2</sub>O conversion was observed after the addition of NO<sub>x</sub> (0.35 mole %) to the gas mixture containing 0.1 mole % N<sub>2</sub>O, 5 mole % O<sub>2</sub> and 2 mole % H<sub>2</sub>O in N<sub>2</sub>O decomposition over Co<sub>4</sub>MnAl catalyst. For that reason, the simulated process stream contained only 0.1 mole % N<sub>2</sub>O, 5 mole % O<sub>2</sub> and 2 mole % H<sub>2</sub>O balanced by N<sub>2</sub> was used for calculation. The first-order rate law was applied to the kinetics of N<sub>2</sub>O decomposition at atmospheric pressure in this simulated stream over the cylinder extrudates (3 × 3 mm) from fresh Co<sub>4</sub>MnAl<sup>50</sup>. The model of reactor consist of equations described below<sup>51,52</sup>.

Material balance of component A (A = N<sub>2</sub>O) in differential dimension dz of plug flow reactor operating in steady state:

$$\dot{n}_A^o \frac{dX_A}{dz} = -r_A A \rho_b \cdot \quad (2)$$

Kinetic equation for first-order rate law including the internal and external mass transfer limitations described by effectiveness factor  $\Omega$ :

$$r = -r_A = \Omega 89859 e^{\frac{-137181}{RT}} c_A . \quad (3)$$

Concentration of component A using conversion  $X_A$  and neglecting the change of volumetric flow along the reactor:

$$c_A = c_{A0} (1 - X_A) \frac{p}{p_0} . \quad (4)$$

TABLE III  
Parameters of the model operating reactor unit

Input parameter	Value	Calculated parameter	Value <sup>a</sup>
Inlet pressure	130 000 Pa	Bed height	2.8 m
Inlet temperature	450 °C	Catalyst bed volume	35 m <sup>3</sup>
Flow rate	30 000 m <sup>3</sup> h <sup>-1</sup> (NTP)	Catalyst weight	28 t
Reactor diameter	4 m	Pressure drop	2.7 × 10 <sup>4</sup> Pa
Specific surface area of catalyst	93 m <sup>2</sup> g <sup>-1</sup>	Effective diffusion of N <sub>2</sub> O	1.77 × 10 <sup>-7</sup> m <sup>2</sup> s <sup>-1</sup>
Catalyst bed density	1290 kg m <sup>-3</sup>	Mass transfer coefficient	0.03 m s <sup>-1</sup>
Equivalent particle diameter (cylinder 3 × 3 mm)	0.0037 m	Internal effectiveness factor	0.15
Pore diameter, (average)	9 × 10 <sup>-9</sup> m	Overall effectiveness factor	0.14
Catalyst bed porosity	0.38		
Rate constant (1st rate)	1.102 × 10 <sup>-5</sup> m <sup>3</sup> s <sup>-1</sup> g <sup>-1</sup>		
Density of waste gas at the inlet	0.512 kg m <sup>-3</sup>		
Dynamic viscosity of waste gas	0.295 × 10 <sup>-4</sup> Pa s		

<sup>a</sup> Calculated for 90% N<sub>2</sub>O conversion.

Pressure lost in the fixed bed:

$$\frac{dp}{dz} = \frac{2c_D \rho v^2}{dp} \quad (5)$$

Where  $c_D$  is resistance coefficient according to Ergun equation:

$$c_D = \frac{1 - \varepsilon}{\varepsilon} \left[ \frac{150(1 - \varepsilon)}{Re} + 1.75 \right] \quad (6)$$

Inlet and calculated parameters of the operating reactor unit are given in Table III.

The estimated volume of the catalytic bed necessary for 90%  $N_2O$  conversion is quite high. Thus, further research will be focused on an increase in catalyst activity, especially in the presence of water vapor as well as on experimental ascertainment of the pressure effect on the kinetics of  $N_2O$  decomposition. The reaction is hindered by internal diffusion in catalyst pores, as it is evident from the value of the internal effectiveness factor. That is why attention will be also focused on optimization of the size and shape of catalyst particles with the aim to decrease the effect of internal mass transport at acceptable pressure drop.

#### LIST OF SYMBOLS

$A$	cross-section of reactor, $m^2$
$c_A$	concentration of compound A, $mol\ m^{-3}$
$c_{A0}$	inlet concentration of compound A, $mol\ m^{-3}$
$c_D$	resistance coefficient
$\dot{n}_A^0$	inlet molar flow of compound A, $mol\ s^{-1}$
$p$	total pressure, Pa
$p_0$	inlet total pressure, Pa
$R$	universal gas constant, $J\ mol^{-1}\ K^{-1}$
$r$	reaction rate, $mol\ s^{-1}\ g^{-1}$
$-r_A$	rate of increment of compound A, $mol\ s^{-1}\ g^{-1}$
$Re$	Reynolds number
$T$	thermodynamic temperature, K
$X_A$	conversion of compound A
$\varepsilon$	porosity of the catalyst bed
$\rho$	gas density, $kg\ m^{-3}$
$\rho_b$	density of the catalyst bed, $kg\ m^{-3}$
$\Omega$	overall effectiveness factor
$\nu$	kinematic viscosity, $m^2\ s^{-1}$

This work was supported by the Ministry of Education, Youth and Sports of the Czech Republic (MSM 6198910016 and MSM 6046137302). The authors thank Z. Bastl (J. Heyrovský Institute of Physical Chemistry, Academy of Sciences of the Czech Republic, v.v.i., Prague) for performing the XPS analysis.

## REFERENCES

1. Pérez-Ramírez J., Kapteijn F., Schöffel K., Moulijn J. A.: *Appl. Catal., B* **2003**, *44*, 117.
2. Kraft J., Bátorla R.: *Výroba kyseliny dusičné*, p. 22. SNTL, Praha 1962.
3. *Best Available Technologies – BAT*, Vol. 8, Appendix, 2002, European Commission; <http://www.ipcc.cz/soubory/velanorch/index.html>, downloaded 15. 10. 2006.
4. Kapteijn F., Rodriguez-Mirasol J., Moulijn J. A.: *Appl. Catal., B* **1996**, *9*, 25.
5. Angelidis T. N., Tzitzios V.: *Ind. Eng. Chem. Res.* **2003**, *42*, 2996.
6. Tanaka K., Shimizu A., Fujimori M., Kodama S., Sawai S.: *Bull. Chem. Soc. Jpn.* **2003**, *76*, 651.
7. Marnellos G. E., Efthimiadis E. A., Vasalos I. A.: *Appl. Catal., B* **2003**, *46*, 423.
8. Mauvezin M., Delahay G., Coq B., Kieger S.: *Appl. Catal., B* **1999**, *23*, L79.
9. Brink R. W., Booneveld S., Pels J. R., Bakker D. F., Verhaak M. J. F. M.: *Appl. Catal., B* **2001**, *32*, 73.
10. Boutarouch M. N., Cortés J. M. G., Begrani M. S. E., Lecea C. S. M., Pérez-Ramírez J.: *Appl. Catal., B* **2004**, *54*, 115.
11. Ruiz-Martínez E., Sánchez-Hervás J. M., Otero-Ruiz J.: *Appl. Catal., B* **2004**, *50*, 195.
12. Vargas A. G., Delahay G., Coq B.: *Appl. Catal., B* **2003**, *42*, 369.
13. Coq B., Mauvezin M., Delahay G., Kieger S.: *J. Catal.* **2000**, *195*, 298.
14. Brink R. W., Booneveld S., Verhaak M. J. F. M., Brujin F. A.: *Catal. Today* **2002**, *75*, 227.
15. Delahay G., Mauvezin M., Guzmán-Vargas A., Coq B.: *Catal. Commun.* **2002**, *3*, 385.
16. Delahay G., Mauvezin M., Coq B., Kieger S.: *J. Catal.* **2001**, *202*, 156.
17. Yoshida M., Nobukawa T., Ito S., Tomishige K., Kunimori K.: *J. Catal.* **2004**, *23*, 454.
18. Satsuma A., Maeshima H., Watanabe K., Suzuki K., Hattori T.: *Catal. Today* **2000**, *63*, 347.
19. Cant N. W., Chambers D. C., Yoshinaga Y.: *Catal. Commun.* **2004**, *5*, 625.
20. Christoforou S. C., Efthimiadis E. A., Vasalos I. A.: *Catal. Lett.* **2002**, *79*, 137.
21. Pérez-Ramírez J., Garcia-Cortés J. M., Kapteijn F., Illán-Gómez M. J., Ribera A., Leccea C. S. M., Moulijn J. A.: *Appl. Catal., B* **2000**, *25*, 191.
22. Coq B., Mauvezin M., Delahay G., Butet J. B., Kieger S.: *Appl. Catal., B* **2000**, *27*, 193.
23. Obalová L., Bernauer B.: *Chem. Listy* **2003**, *5*, 255.
24. Kannan S., Swamy C. S.: *J. Mater. Sci. Lett.* **1992**, *11*, 1585.
25. Pérez-Ramírez J., Kapteijn F., Moulijn J. A.: *Appl. Catal., B* **1999**, *23*, 59.
26. Kannan S., Swamy C. S.: *Catal. Today* **1999**, *53*, 725.
27. Kloprogge J. T., Frost R. L.: *Appl. Catal., A* **2000**, *204*, 269.
28. Pérez-Ramírez J., Mul G., Xu X., Kapteijn F., Moulijn J. A.: *Appl. Catal., A* **2000**, *204*, 265.
29. Pérez-Ramírez J., Mul G., Xu X., Kapteijn F., Moulijn J. A.: *J. Mater. Chem.* **2001**, *11*, 821.
30. Jitianu M., Balasoiu M., Marchidan R., Zaharescu M., Crisan D., Craiu M.: *Int. J. Inorg. Mater.* **2000**, *2*, 287.

31. Barriga C., Fernandez J. M., Ulibarri M. A., Labajos F. M., Rives V.: *J. Solid State Chem.* **1996**, 124, 205.
32. Kannan S., Swamy C. S.: *Catal. Today* **1999**, 53, 725.
33. Pérez-Ramírez J., Kapteijn F., Moulijn J. A.: *Catal. Lett.* **1999**, 60, 133.
34. Kannan S.: *Appl. Clay Sci.* **1998**, 13, 347.
35. Farris T. S., Li Z., Armor J. N., Braymer T. A.: U.S. 5 472 677 (1995); *Chem. Abstr.* **1996**, 124, 96122u.
36. Kannan S., Swamy C. S.: *Appl. Catal., B* **1994**, 3, 109.
37. Chang K. S., Song H., Park Y. S., Woo J. W.: *Appl. Catal., A* **2004**, 273, 223.
38. Román-Martínez M. C., Kapteijn F., Cazorla-Amorós D., Pérez-Ramírez J., Moulijn J. A.: *Appl. Catal., A* **2002**, 225, 87.
39. Pérez-Ramírez J., García-Cortés J. M., Kapteijn F., Illán-Gómez M. J., Ribera A., Salinas-Martínez de Lecea C., Moulijn J. A.: *Appl. Catal., B* **2000**, 25, 191.
40. Pérez-Ramírez J., Mul G., Xu X., Kapteijn F., Moulijn J. A.: *Stud. Surf. Sci. Catal.* **2000**, 130, 1445.
41. Kustrowski P., Chmielarz L., Rafalska-Lasocha A., Dudek B., Wegrzyn A., Dziembaj R.: *Przem. Chem.* **2003**, 82, 732.
42. Obalová L., Jiráťová K., Kovanda F., Valášková M., Balabánová J., Pacultová K.: *J. Mol. Catal. A* **2006**, 248, 210.
43. Obalová L., Jiráťová K., Kovanda F., Pacultová K., Lacný Z., Mikulová Z.: *Appl. Catal., B* **2005**, 60, 297.
44. Obalová L., Pacultová K., Balabánová J., Jiráťová K., Bastl Z., Valášková M., Lacný Z., Kovanda F.: *Catal. Today* **2007**, 119, 233.
45. Kovanda F., Rojka T., Dobešová J., Machovič V., Bezdička P., Obalová L., Jiráťová K., Grygar T.: *J. Solid State Chem.* **2006**, 179, 812.
46. Kovanda F., Grygar T., Dorničák V.: *Solid State Sci.* **2003**, 5, 1019.
47. Kannan S.: *Appl. Clay Sci.* **1998**, 13, 347.
48. Swamy C. S., Kannan S., Li Z., Armor J. N., Braymer T. A.: U.S. 5 407 652 (1995); *Chem. Abstr.* **1995**, 122, 247133k.
49. Pacultová K.: *Ph.D. Thesis*. Technical University of Ostrava, Ostrava 2007.
50. Obalová L.: *Habilitation Thesis*. Technical University of Ostrava, Ostrava 2005.
51. Fogler H. S.: *Elements of Chemical Reaction Engineering*, 3rd ed. Prentice Hall PTR, New Jersey 1999.
52. Dítl P.: *Chemické reaktory*, 2. vydání. Vydavatelství ČVUT, Praha 2000.